Article ID: 1001-3555(2014)05-0436-14

The Photocatalytic and Thermal Catalytic Reduction of CO_2 with H_2 over Pt/TiO_2 Catalysts

CHEN Shu-qing [1,2], LV Gong-xuan [1*]

(1. *State Key Laboratory for Oxo Synthesis and Selective Oxidation, Lanzhou Institute of Chemical Physics, Chinese Academy of Sciences, Lanzhou* 730000, *China*;
2. *University of Chinese Academy of Sciences, Beijing* 100049, *China*)

Abstract: Pt/TiO_2 with Pt loading ranging from 0.5 to 2% were prepared by wet impregnation method. CO_2 hydrogenation over Pt/TiO_2 was investigated under light irradiation and thermal conditions respectively. Results indicated hydrogenation of CO_2 could be catalyzed by Pt/TiO_2 under both conditions, but the reaction occurred in the different ways. Under thermal condition, CO_2 was converted to CO and CH_4, the main product was CO at low temperature (100% of CO selectivity at 250 ℃ over 0.5% Pt/TiO_2). Increase of reaction temperature led to increase of CH_4 selectivity from 0 to 60.94% when reaction temperature rose from 250 to 450 ℃ over 1.5% Pt/TiO_2. The increase of Pt loading also resulted in the increase of CH_4 selectivity. On the contrary, CH_4 was the only product under light irradiation. The CO_2-TPD results indicated Pt served as CO_2 adsorption centers. CO_2 adsorbed on Pt site *via* carbonyl group. Under light irradiation, excited electrons were trapped by Pt and reduced surface adsorbed carbonyl species to form CH_4 *via* formic acid intermediate. However, under thermal condition, H_2 was first decomposed into H atoms over Pt, then reduced the carbonyl species adsorbed on Pt to form CO, and hydrogenated CO to produce CH_4.

Key words: photocatalytic; thermal catalytic; CO_2 hydrogenation

CLC number: O643.32 **Document code**: A

Nowadays, with the fast development of industry and economy, traditional energies are confronted with depletion and global warming problems caused mainly by CO_2 emission have become a serious problem affecting the ecosystem[1-5]. CO_2 hydrogenation has been regarded as one of the most promising method solving this problem if the driving power is provided by sustainable energy[6-9].

So far, CO_2 hydrogenation is usually investigated under thermal and light irradiation conditions. The photocatalytic reduction of CO_2 attracts extensive attention since it can be driven by inexhaustible solar energy, forming some valuable chemicals, such as methanol or methane, under mild conditions[10]. Many efforts have been made to develop highly efficient photocatalysts for the photocatalytic reduction of CO_2, including noble metal loading[11-15], doping[16-18], coupling[19-21], changing the morphology of supports[22-26] and addition of co-catalysts[27]. However, mechanism of photocatalytic CO_2 hydrogenation still remains unclear. Lo et al.[28] investigated photoreduction of carbon dioxide with H_2 over TiO_2 and ZrO_2. They proposed that CO_2 reacted with $\cdot H$ from H_2 to form HCOOH, and then dehydration of HCOOH to HCOH proceeded *via* reaction with $\cdot H$. Followed by further dehydration of HCOH with $\cdot H$ to $\cdot CH_3$, $\cdot CH_3$ reacted with $\cdot H$ to form CH_4 and C_2H_6. Zhang et al.[29] proposed a possible pathway for photocatalytic reduction of CO_2 with gaseous H_2O to generate CH_4 on Pt/TiO_2 catalyst. Photo-generated electron transferred to Ti center to form excited state $[Ti^{3+}\text{-}O]^*$ species, and the excited hole h^+ oxidized H_2O to $\cdot OH$ and

Received date: 2014-04-11; **Revised date**: 2014-05-04.

Foundation: This work was supported by the National Sciences Foundation of China(21433007,21173242).

First author: Shu-qing, Chen(1985), Master, Female, chenshuqing139@163.com.

* **Corresponding author**: 0931-4968178, gxlu@lzb.ac.cn.

H^+, and OH radicals further oxidized h^+ and H_2O to O_2 and H^+. CO_2 dissociated to CO and O_2 *via* reaction with $[Ti^{3+}\text{-}O]^*$ species, and CO could generate ·C and O_2. Finally, ·C reacted with H^+ and e^- to form CH_4. However, Yu et al.[30] suggested that the dissociative adsorption of CO_2 or the reduction of CO_2 with H_2 led to the formation of CO. Then CO is hydrogenated to produce CH_4.

Unlike photocatalytic reaction, CO_2 hydrogenation under the thermal condition refers to reduce CO_2 under high temperature and sometimes even high pressure. In order to obtain better activity and selectivity, it usually needs rigorous conditions and huge energy consumption. To overcome these problems, hydrogenation of CO_2 has been intensively investigated by promotion *via* metal loading[31-32], support modification[30, 33-35], development of catalysts preparation methods[36-37] and co-catalysts[38]. Up to date, two major mechanisms of CO_2 hydrogenation under the thermal condition have been proposed. One involves CO_2 first dissociation into CO and then CO hydrogenation to form methane. Over $Rh/\gamma\text{-}Al_2O_3$ catalyst at low temperature and atmospheric pressure, CO_2 first chemisorbs on the surface, and then dissociates into CO and O. Finally, CO and O react with H_2 to produce CH_4 and H_2O[39]. Marwood et al[40] investigated reaction intermediates of CO_2 methanation over Ru/TiO_2 catalyst *via* steady-state transient measurements. Results indicate that CO and formate are main intermediates. Here, CO is a key intermediate which hydrogenates to form CH_4, while formate is only intermediate to produce CO. Another is that CO_2 reacts with hydrogen to generate methane without forming CO as intermediate. CO_2 rapidly adsorbs on the surface of the catalysts and then is reduced to surface formate[41]. Subsequently, surface formate reacts with hydrogen to form methane directly.

Even though much effort has been devoted to the heterogeneous reduction of CO_2 and great progress has been achieved in both the activity and selectivity of the catalysts, mechanisms of catalytic hydrogenation of CO_2 are still controversial. At the same time the effect of reaction conditions on selectivity of the products is unknown. In tis paper, the CO_2 hydrogenation under thermal and irradiation conditions were conducted over Pt/TiO_2 separately. The selectivity difference of products under different reaction conditions was focused and the reasons for this difference were discovered. Our work allow us to deeply understand the influence of reaction conditions on selectivity of products in CO_2 hydrogenation, and afford new ideas to design better catalysts for CO_2 hydrogenation. Under the thermal condition, CO_2 was converted to CO and CH_4, the main product was CO at low temperature (100% of CO selectivity at 250 ℃ over 0.5% Pt/TiO_2 catalyst). Increase of reaction temperature led to increase of selectivity to CH_4 from 0 to 60.94% when reaction temperature rose from 250 to 450 ℃ over 1.5% Pt/TiO_2 catalyst. The increase of Pt loading also resulted in the increase of selectivity of CH_4. On the contrary, methane was the only product under irradiation condition. The possible photo and thermal reaction mechanism were discussed.

1 Material and methods

1.1 Catalyst synthesis

Commercial P25 TiO_2[42-43] (specific surface area of 50 $m^2 g^{-1}$, the weight ratio of anatase to rutile is 70 to 30%) from Degussa was used as received. All other chemicals used in this work were AR reagents. TiO_2 was prepared by the hydrothermal method[44]. Briefly, 5 g PVP (polyvinylpyrrolidone, average molecular weight 10 000) powder was dissolved with 18 mL of absolute ethanol. Subsequently, 15 g tetrabutyl titanate was added into the above mixture, and magnetic stirring for 1 h under ambient temperature. Afterwards, a mixture of 30 mL distilled water and 11 mL absolute ethanol was added into the above results dropwise and magnetic stirring for 2 h under ambient temperature. Then the mixture was placed in a 100 mL Teflon-lined stainless steel autoclave and heated at 130 ℃ for 24 h. The obtained suspensions were extracted filtration and washed by ethanol and water several times. The catalysts were dried at 100 ℃ and to evaporate water, followed by calcined at 400 ℃ for 3 h to obtain the hydrothermally synthesized TiO_2 powders, named

TiO_2(HT).

TiO_2 supported Pt catalysts (Pt/TiO_2) with Pt loading ranging from 0.5% to 2% were prepared by wet impregnation method according to reference[45]. A certain amount of hexa chloro platinic acid solution ($H_2PtCl_6 \cdot 6H_2O$) was taken based on Pt content in the sample (0.5% ~2.0%). It was then mixed with 2 g P25. The resulting slurry was stirred at ambient temperature for 24 h and dried at 120 ℃ for 24 h to evaporate the water completely. The solid residue was calcined in air at 450 ℃ for 3 h. Prior to the CO_2 (CO) photo and thermal catalytic reduction reaction, the calcined catalysts were reduced at T = 450 ℃ (heating rate 10 ℃/min) for 3 h, under a 50% H_2 in N_2 stream (flow rate 60 mL/min). P25 supported Pt is entitled Pt/P25 in the experiment. Pt loaded on TiO_2 synthesized by the hydrothermal method is denoted as Pt/TiO_2(HT).

1.2 Catalyst characterization

The X-ray diffraction patterns (XRD) of samples were recorded to verify the species in the catalysts on an X´Pert Pro multipurpose diffractometer (PANalytical, Inc.) using Cu K α radiation in the scanning angle range of 15° ~85° at 40 mA and 40 kV. Transmission electron microscopy(TEM) images were taken with a Tecnai-G2-F30 field emission transmission electron microscope operating at an accelerating voltage of 300 kV. The samples were dispersed in absolute ethanol by moderate sonication. A Lacy carbon-coated 200 mesh TEM micro-grid was dipped into the sample suspension and then dried under vacuum at given temperature for a while prior to analysis.

The nitrogen adsorption and desorption isotherms at −196 ℃ were performed on an adsorption apparatus (Micromeritics ASAP 2020 M). Prior to the tests, samples were degassed at 110 ℃ for 4 h. The specific surface areas were calculated *via* the BET method in the relative pressure range of 0.05 ~0.3. UV-VIS diffuse reflectance spectra were obtained with a Shimadzu UV-3600 UV-VIS-near-IR spectrophotometer. $BaSO_4$ was used as a reflectance standard. Thermogravimetric-different scanning calorimetry (TG-DSC) measurements were carried out on a NETZSCH STA 449F3 thermogravimetric analyzer from room temperature to 800 ℃ with the rate of 10 ℃/min under air atmosphere. X-ray photoelectron spectroscopy (XPS) analysis was performed using a VG Scientific ESCALAB210-XPS photoelectron spectrometer with a Mg Kα X-ray resource. CO_2 temperature programmed desorption (TPD) measurements were carried out on an AMI-100 unit (Zeton-Altamira instrument). The sample (100 mg) was pretreated at 200 ℃ for 15 min in a He stream (50 mL/min). After being cooled down to 20 ℃, the pretreated sample was exposed in CO_2 atmosphere for 40 min. Then the sample was purged with He gas stream at 20 ℃ until the baseline of CO_2 in the mass spectrum was steady. Finally, the CO_2-TPD was carried out with a ramp of 20 ℃/min from 20 ℃ to the needed temperature under He stream.

1.3 Catalytic activity

Photocatalytic reduction of CO_2 with H_2 was performed in a sealed quartz flask[46] (about 120 mL) with a flat window (an efficient irradiation area of about 12 cm^2) under ambient conditions and using 200 W Hg lamp as light source. In a typical photocatalytic experiment, 0.3 g reduced Pt/P25 (0.5% ~2.0%) was added into the flask and degassed by bubbling Ar gas for 40 min prior to the introduction of the reactant gases (i.e., CO_2 and H_2). Before light irradiation, 10 mL high purity CO_2 and 40 mL H_2 were led into the photoreduction system. Photocatalytic reduction of CO with H_2 was similar to that of CO_2 except that 30 mL H_2 was introduced into the CO photoreduction system. In our photoreduction experiments, methane was detected as the only gas product by gas chromatography. The product mixtures were analyzed on a GC112A gas chromatography equipped with a capillary pora-Q column (30 m×0.53 mm×10 μm) and a flame ionization (FID) detector using N_2 as gas carrier[47].

CO_2 hydrogenation under the thermal condition was carried out in a fixed-bed continuous flow quartz reactor (i.d. 8 mm) at atmospheric pressure and in the temperature range of 250 to 500 ℃. Typically, 0.3 g of catalyst (0.5% ~2.0%) was used in each run and H_2/CO_2 mixture (4∶1) were introduced into the catalyst bed at a total flow rate of 50 mL/min using

N_2(30 mL/min) as the carrier gas and internal standard for gas analysis. The separation and quantification of the gas phase effluents were realized on two on-line chromatographies equipped with thermal-conductivity detectors (TCD). In our experiments, both methane and CO were detected as the gas products by gas chromatography. Thermal catalytic activity was defined in terms of conversions of CO_2 and selectivity to the products. The conversions of CO_2 were denoted as CO_2 conversion in the figures. While the selectivity to the products (CH_4, CO) were denoted as $S_{product}$, which were calculated according to the corresponding equations: S(CO) (%) = 100×(moles of CO production)/(moles of CO_2 consumed); the calculated method of S(CH_4) were similar to that of S(CO). However, CO hydrogenation was similar to CO_2 hydrogenation except that CO was introduced into the system instead of CO_2 and H_2/CO molar ratio was 3.

2 Results and conclusions

2.1 Catalyst characterization

2.1.1 XRD analysis　Powder X-ray diffraction analysis (Fig. 1) shows the XRD patterns of Pt/P25 (0.5% ~2.0%) and 0.5% Pt/TiO_2(HT) catalysts reduced at 450 ℃. The peaks at 2θ = 25.3°, 37.9°,

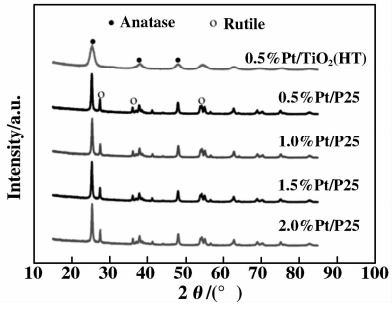

Fig. 1 XRD patterns of 0.5% ~2% Pt/P25 and Pt/TiO_2(HT) samples

48° are identified as anatase phase of TiO_2, and the other diffraction peaks at 2θ = 27.4°, 36°, 41.2° are representative of rutile phase of TiO_2 structure, which coincides exactly with the reference[29, 42, 48-49]. These results show that the P25 TiO_2 consists of both anatase and rutile, while TiO_2(HT) exists only in anatase phase[44]. However, no detectable crystallite of Pt species can be observed in either Pt/P25 or Pt/TiO_2(HT) catalysts. The absence of diffraction lines in the Pt phase for the Pt supported catalysts is probably due to the high dispersion of Pt. From Fig. 1, it can be seen that loading Pt does not change the phase of P25. The crystallite size of the Pt/P25 samples calculated by the Scherrer's formula is found out to be 34 nm. The mass fraction of anatase phase (FA) is calculated *via* the usually accepted quantitative method[49-50] as Eq. (1) with the strongest peak intensity IA and IR of the anatase (101) crystal face and the rutile (110) crystal face, respectively. According to equation (1), the content of anatase phase in the P25 TiO_2 sample is 72.09%, which is close to 70%[42]. This difference could be caused by the combination effect of loading Pt on P25 and calculation of the Pt/P25 at high temperature. The crystallite size of the Pt/TiO_2(HT) samples is calculated to be 30 nm. Smaller size of Pt/TiO_2(HT) than Pt/P25 broadens the XRD peaks of Pt/TiO_2(HT).

$$FA = \frac{1}{1+1.26(IR/IA)} \quad (1)$$

2.1.2 TEM analysis　TEM analysis is performed to investigate the morphology of Pt/P25 (0.5% ~ 2.0%) reduced at 450 ℃ for 3 h; and the result is displayed in Fig. 2. As shown in Fig. 2, small dark spots on the TiO_2 particles represent the Pt-metal particles. It clearly demonstrates that Pt particles are small and uniformly dispersed throughout the support P25 TiO_2[31]. It is also observed that average sizes of 0.5%, 1.0%, 1.5%, 2.0% Pt/P25 are 1.35, 1.8, 2.4, 3.65 nm, respec-tively. Moreover, no obvious

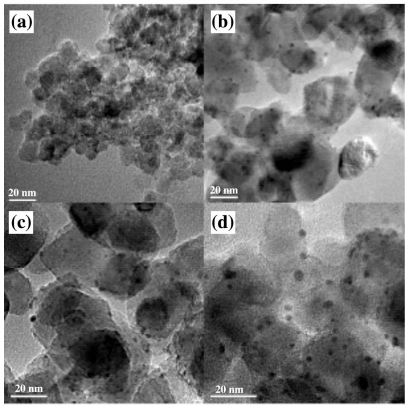

Fig. 2 TEM images of the reduced 0.5% ~2.0% (weight percentage) Pt/P25 powders

agglomeration phenomenon is observed at the Pt sites. A high dispersion of Pt species might be due to the high surface area of the P25 TiO_2 and the low Pt loading. As shown in the XRD picture Fig. 1, it is supposed that the high dispersion of Pt species probably leads to the absence of diffraction lines in the Pt phase for the Pt supported catalysts[29]. The high dispersion of Pt might result in a good activity of CO_2 hydrogenation.

2.1.3 N_2 adsorption-desorption analysis The BET surface area, volume of pores and average pore diameter of P25, Pt/P25(0.5% ~2.0%), TiO_2(HT) and 0.5% Pt/TiO_2(HT) catalysts are displayed in Table 1.

Table 1 Physicochemical properties of the supports and Pt catalysts reduced at 450 ℃

Catalyst	Metal loading /(wt. %)	S_{BET} /($m^2 \cdot g^{-1}$)	V_{pore} /($cm^3 \cdot g^{-1}$)	d_{pore} /nm
TiO_2(HT)	–	118.4	0.32	10.7
Pt/TiO_2(HT)	0.5	132.8	0.29	8.7
P25	–	50.5	0.54	44.4
Pt/P25	0.5	48.9	0.31	24.7
Pt/P25	1.0	47.1	0.29	24.4
Pt/P25	1.5	47.4	0.24	20.2
Pt/P25	2.0	47.7	0.21	17.3

The BET surface area of the support P25 is close to 50 $m^2 \cdot g^{-1}$, which accords with the real character of commercial P25[42]. All the surface areas of Pt/P25 (0.5% ~2.0%) are a little smaller than that of P25, which might arise from the impregnation of Pt. It is indicated that loading Pt does not lead to any evident structural changes of the support P25. It is also the case with TiO_2(HT) and 0.5% Pt/TiO_2(HT) catalysts. According to Table 1, Pt/TiO_2(HT) has large surface area more than twice as that of Pt/P25 catalyst. Generally speaking, larger surface area can provide more active sites. The relationship between surface area and activity will be discussed in the next section.

2.1.4 UV-vis diffuse reflectance spectra analysis

Fig. 3 shows the UV-VIS absorption spectra for P25, TiO_2(HT), 0.5% Pt/P25 and 0.5% Pt/TiO_2(HT) catalysts reduced at 450 ℃. The P25 TiO_2 absorbs light of wavelength below 400 nm because of its wide band gap energy. Compared to the support P25, Pt/P25 has a similar absorption, but it shows a slightly red-shift in the spectrum[48], which is attributed to the light absorption of Pt metals on the surface of support P25 TiO_2. Whereas, the absorption edge of Pt/TiO_2 (HT) is almost in the same position as that of TiO_2 (HT). According to Fig. 3, It shows that Pt/P25 has a stronger absorption than Pt/TiO_2 (HT) at wavelengths less than 400 nm, and a little red-shift in the spectrum (λ>400 nm). Stronger absorption in the UV spectrum indicates a good light harvesting for UV light, which suggests Pt/P25 is more likely to have an enhanced photocatalytic activity than Pt/TiO_2(HT).

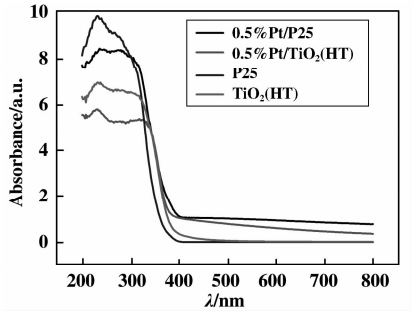

Fig. 3 UV/Vis diffuse reflectance spectra for P25, TiO_2(HT), 0.5% Pt/P25 and Pt/TiO_2(HT)

2.1.5 TG-DSC analysis The TG-DSC curve of TiO_2(HT) prepared by the hydrothermal method and dried at 100 ℃ for 2 h is represented in Fig. 4. As observed in the figure, there is an endothermic peak and an exothermic peak in the curve. The narrow and weak endothermic peak at 58 ℃ or which extends to 80 ℃ is attributed to the evaporation of the absorbed water in the sample. The appearance of this peak is due to the

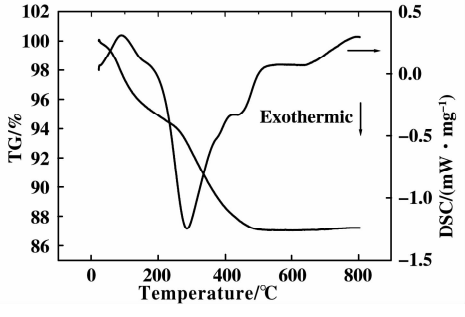

Fig. 4 Thermal analysis (TG-DSC) curves of TiO_2(HT), prepared by hydrothermal method with template with drying for 3h at 100 ℃

fact that TiO_2(HT) is not dried completely. The sharp and strong exothermic peak in the 266 ~ 500 ℃ temperature range is caused by the decomposition of PVP (template agent) left in the sample in the process of the preparation. Therefore, theoretically it could be ensured that most PVP could be removed after calcined at 400 ℃ for 3 h. In fact, due to the encapsulation between the catalyst particles, a small amount of PVP is left inevitably in the TiO_2(HT) after calcined. Then residual PVP particles might act as defective sites to affect the activity of the catalyst.

2.1.6 XPS analysis　The chemical state of Pt nanoparticles on Pt/P25 (0.5% ~2.0%) reduced at 450 ℃ is investigated and confirmed by XPS, and the results are shown in Fig. 5. For Pt/P25 with different Pt loading, it can be found that the binding energies of Pt $4f_{7/2}$ and $4f_{5/2}$ electrons are all at about 70.9 and 74.2 eV, respectively, which can be assigned to Pt^0 based on the standard binding energy data[51-53]. In addition, co-existence of neither Pt^{2+} nor Pt^{4+} is observed. Accordingly, the Pt particles on Pt/P25 are all in the metallic state, Pt^0. Thus, it can be concluded that Pt oxides species loaded on the support P 2 5 TiO_2 are completely reduced by H_2. To the best of our knowledge, noble metal loaded on the support is usually used for hydrogenation catalysts because of its feature in dissociating H_2[7]. In our study, Pt metal supported on P25 is regarded as one of the active components for CO_2 hydrogenation.

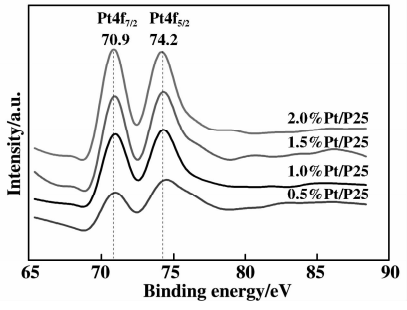

Fig. 5 XPS spectra of 0.5-2.0% Pt/P25

2.1.7 CO_2 TPD analysis　Fig. 6 presents the CO_2-TPD profiles of P25 and 0.5% Pt/P25. As shown in Fig. 6, there exist four and five desorption peaks for P25 and Pt/P25, respectively, which means that there are four and five kinds of adsorption centers on the surface of P25 and Pt/P25, respectively. It is known that different CO_2 desorption peaks represent different carbonaceous species. For P25, these four desorption peaks are noted as C1, C2, C3, C4, respectively. After loading Pt on P25, all the four types of desorption don't change significantly, but a new desorption peak appears, which is expressed as C5. Fig. 7 shows possible forms of five kinds of carbonaceous species, which is in good agreement with the studies reported by Katsumi Tanaka[54-55]. Compared the amount of desorbed CO_2 of Pt/P25 with that of P25, there is almost no change for the LT (low-temperature, ~200 ℃) peak and HT (high-temperature, >600 ℃) peak after Pt loading. As a result, it is speculated that LT and HT peak are caused by CO_2 adsorption on the support P25. The clear difference is that Pt loading leads to significant change of MT(medium-temperature, 200 ~ 600 ℃) peaks. It is obvious that the desorbed amount of CO_2 from C2 and C3 is enhanced after the loading of Pt on P25, which is indicated that Pt loading promotes CO_2 adsorption of moderate intensity on P25. It is also

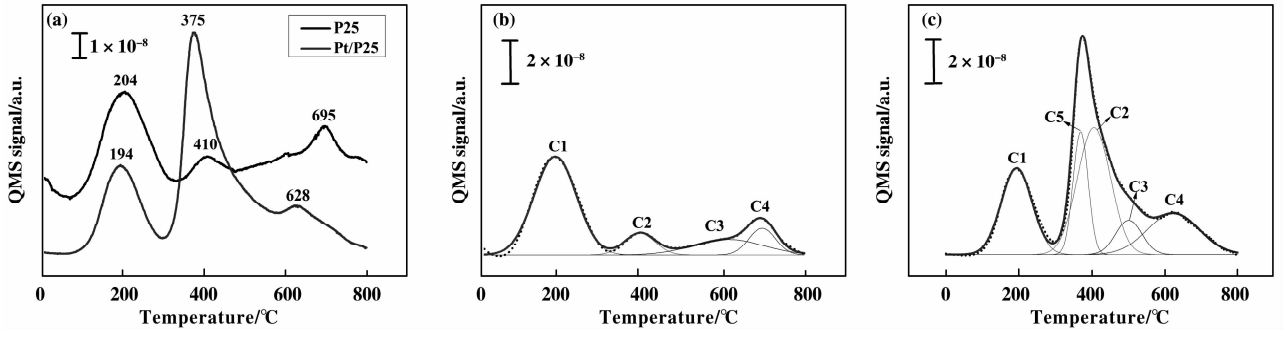

Fig. 6 a. CO_2-TPD profiles of P25 and 0.5% Pt/P25, b. The deconvolution of CO_2-TPD on P25.
c. The deconvolution of CO_2-TPD on 0.5% Pt/P25.

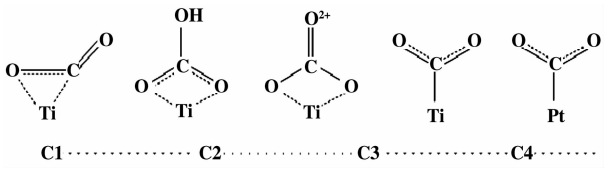

Fig. 7 Possible forms of CO_2 adsorption on P25 and 0.5% Pt/P25

observed that C5 appears after Pt loading. Therefore, it suggests that the Pt particles supported on the P25 could act as adsorption centers to form C5, leading to a higher capacity of CO_2 adsorption[30]. This phenomenon might arise from the dissociative adsorption of CO_2 on the Pt/P25[54-55]. In addition, C3 and C4 desorption peak maximum of Pt/P25 as compared to the support P25 move toward lower temperature direction in Fig. 6, which might be caused by Pt loading. The lower CO_2 desorption temperatures are due to the weaker adsorption of CO_2 on the P25, which is caused by the strong interaction of Pt and the support.

2.2 Activity experiment

2.2.1 Photocatalytic activity A series of blank experiments are performed. No product is detected under dark conditions or under UV irradiation without the photocatalyst when the other reaction conditions remain the same. This indicates that the presence of both photocatalyst and UV irradiation is necessary for CO_2 hydrogenation. In addition, CH_4 is not detected without CO_2 as the reactant, confirming that CH_4 is derived from CO_2.

2.2.1.1 Comparison of Pt/P25 and Pt/TiO_2(HT) as catalyst for CO_2 photocatalytic reduction In our photo experiment, P25 (TiO_2(HT)) is inactive in photocatalytic reduction of CO_2 with H_2. However, Pt/P25 (Pt/TiO_2(HT)) promotes drastically the reduction of CO_2 with H_2[29, 56]. This suggests Pt particles are important active sites. Owing to the higher work function of Pt-metal than TiO_2, excited electrons transmit from conduction band of TiO_2 to the Pt-metal and the holes still stay in the valance band of TiO_2. Therefore, the recombination between electrons and holes is effectively suppressed. The increased electron density on the Pt particles may be in favor of the formation of CH_4, which requires eight electrons.

Fig. 8 shows the variation of CH_4 yield with UV irradiation time over 0.5% Pt/P25 and Pt/TiO_2(HT) reduced at 450 ℃. The CH_4 yields on both photocatalysts increase with the increase of the UV irradiation time, and accumulate to about 23.81 and 5.52 μmol · g^{-1} for Pt/P25 and Pt/TiO_2(HT) under the UV light of 144 h, respectively. It can be obviously found that Pt/P25 enhances the amount of CH_4 evolution by a factor of 3.3 compared to Pt/TiO_2(HT).

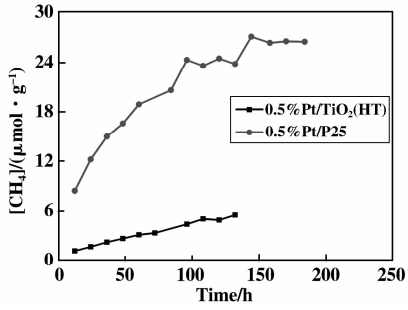

Fig. 8 Variation of CH_4 yield with UV irradiation time over 0.5% Pt/P25 and Pt/TiO_2(HT) at ambient temperature, H_2/CO_2 = 4 : 1

Three factors may affect the activity of the two catalysts. First of all, light adsorption is an important factor. Although the BET surface area of Pt/TiO_2(HT) is more than twice as large as Pt/P25, Pt/P25 has a stronger adsorption of ultraviolet light than Pt/TiO_2(HT). It indicates that specific surface area is not the main factor that affects the activity of photocatalyst, but light adsorption is also an essential aspect. In our experiment, light adsorption seems to be more important. Secondly, XRD results of the two catalysts indicate that P25 is composed of anatase and rutile TiO_2, while TiO_2(HT) contains mainly anatase. To the best of our knowledge, mixed phases of TiO_2 are more active than a single phase of TiO_2. This is because anatase and rutile TiO_2 have different band-gap positions. The former has a more positive conduction band and the latter has a more negative valence band, which results in the fact that photo-generated electrons tend to move to the conduction band of anatase, and the holes remain in the valence band of rutile. This would separate electrons and holes spatially, thus efficiently suppressing the re-

combination of them. Thirdly, the residual template agent PVP in the catalyst may act as the recombination centers for electrons and holes. According to the TG-DSC profile of TiO_2 (HT) (Fig. 4), the template (PVP) could be removed completely *via* the calcination at 400 ℃ for 3 h theoretically. However, some PVP particles might be wrapped around the catalysts particles in the process of preparation. These PVP remaining in the bulk phase of the catalyst become the recombination centers of electrons and holes, thus decreasing the activity of Pt/TiO_2(HT).

2.2.1.2 CO_2 photocatalytic reduction over Pt/P25 (0.5% ~2.0%)　Fig. 9 shows that CH_4 yield in photocatalytic reduction of CO_2 with 0.5% ~ 2.0% loaded Pt-metal on P25. The CH_4 yields on these four photocatalysts all increase with the UV irradiation time, and 1.5% Pt/P25 catalyst exhibits the highest activity on CH_4 yield with 113.51 $\mu mol \cdot g^{-1}$ after 96 h UV irradiation. It is noteworthy that the amount of Pt loading has a great influence on the activity of the catalyst, and a moderate amount of Pt on the P25 can usually improve activity. However, overloaded Pt may serve as recombination center of electron and hole, which is bad for photochemical reaction.

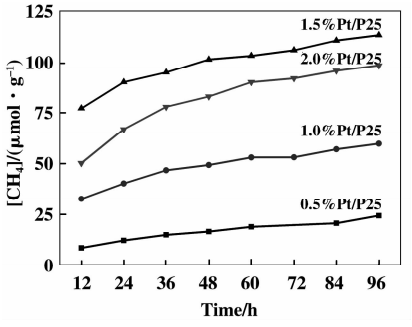

Fig. 9 Variation of CH_4 yield with UV irradiation time over 0.5-2.0% Pt/P25 at ambient temperature, $H_2/CO_2 = 4:1$

2.2.2 Thermal catalytic activity　Fig. 10 shows the conversion of CO_2, selectivity of CH_4 and CO over the Pt/P25 (0.5% ~2.0%) catalyst at reaction temperature from 200 to 500 ℃. As shown in Fig. 10a, an almost linear relationship between CO_2 conversion and temperature is observed. A higher reaction temperature results in a higher conversion of CO_2. In Fig. 10b, for 0.5% Pt/P25, in the range of 250 ~500 ℃, CO selectivity is always larger than 80%, even though it decreases when the temperature is increased. For 1.0% ~ 2.0% Pt/P25, the main product transforms from CO to CH_4 with the increase of the temperature to about 450 ℃. This is due to the increase of Pt loading. Pt particles facilitate a high exposure of active sites, which accelerate the formation of surface-dissociated hydrogen and the subsequent hydrogenation of surface Pt carbonyl species, accounting for the resulting enhanced CH_4 selectivity. At low temperatures (<250 ℃) no formation of CH_4 occurs for 0.5% ~ 1.5% Pt/P25 catalyst as shown in Fig. 10c. An increase in the CH_4 production is also observed with the increase of the temperature. CO methanation is exothermic and will be inhibited theoretically at high temperature. In fact, more CO converts to CH_4 with the increase of temperature because high temperature is beneficial to activate reactants and improve reaction rate. As RWGS is endothermic, more CO will be produced from CO_2 with the increase of the reaction temperature.

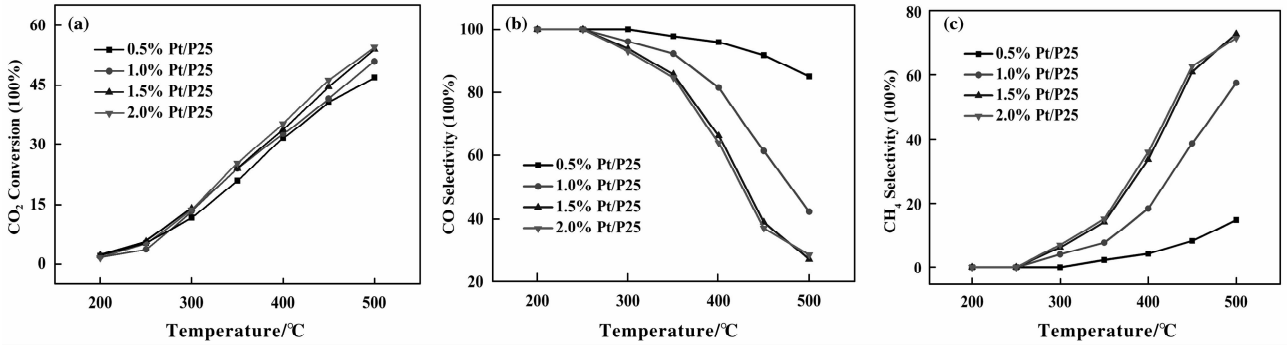

Fig. 10 a. Conversion of CO_2, b. CO selectivity c. CH_4 selectivity over the 0.5-2.0% Pt/P25 catalyst at different temperature. $H_2/CO_2 = 4:1$

In our thermal experiment, P25 is inactive CO_2 hydrogenation under the thermal condition. However, Pt/P25 enhances substantially the reduction of CO_2 with H_2. CO_2-TPD shows that C5 species appears after Pt loading. In CO_2 hydrogenation, unlike CO_2-TPD, in the presence of reductant H_2, active carbonaceous species would transform into specific species. C5 species converts into carbonyl Pt. This indicates that carbonyl Pt are important intermediate precursor, which promotes the activity of Pt/P25.

From the above figures, it is found that compared to CO_2 hydrogenation under the thermal condition, photocatalytic reduction of CO_2 attains totally CH_4, whereas the former obtains CO and CH_4. The main product transforms from CO to CH_4 with the increase of the temperature, the increase of Pt loading also results in the increase of selectivity of CH_4.

2.3 Reaction mechanism

Our results indicated that CO_2 hydrogenation generated CO and CH_4 under the thermal condition. CH_4 selectivity increased with the temperature, and the increase of Pt loading also resulted in the increase of selectivity of CH_4; while methane was the only product under irradiation condition. To explain this difference of product selectivity, it's necessary to study mechanisms of CO_2 hydrogenation. Even though considerable work has been conducted to establish mechanism of CO_2 hydrogenation, so far many researchers still can't reach an agreement on it, especially on the nature of the intermediate. Goguet et al.[57] considered that the interfacial site (Pt and CeO_2) and the reducible CeO_2 site are the main active sites of the Pt/CeO_2 catalyst. It was suggested that the RWGS reaction proceeded *via* mainly surface carbonate intermediates, Pt-carbonyl species and the formate species. Like CeO_2, TiO_2 exhibits redox characteristics as well. According to Kim[31], Pt sites assist in activating the active sites by activating H_2 in the RWGS reaction rather than acting directly as an active site. TiO_2(reducible TiO_2 and Pt-O_v-Ti^{3+} sites) active sites participated directly in the reaction. According to the results of Panagiotopoulou et al.[58-59], the new active sites located at the metal-support interface after Pt loaded on reducible metal oxides like TiO_2 and CeO_2 exhibited exceptional electron-donating properties and promoted the reaction activity. Tanaka et al.[54] investigated the adsorption of CO_2 on TiO_2 and Pt/TiO_2 by Auger electron spectroscopy (AES) and X-ray photoelectron spectroscopy (XPS) in 1984. The dissociation of CO_2 on Pt/TiO_2 was confirmed by the observation of CO adsorbed on Pt. This result implies that CO_2 dissociates into CO and oxygen, after which the oxygen atoms react with adsorbed CO_2 molecules to form CO_3^{2-} species. Lo et al. investigated photoreduction of carbon dioxide with H_2 and H_2O over TiO_2 and ZrO_2[28]. They proposed a possible mechanism for CO_2 photo reduction by H_2.

2.3.1 Photocatalytic CO_2 hydrogenation mechanism

The variation of CH_4 yield of CO hydrogenation with UV irradiation time over 0.5% Pt/P25 is investigated as shown in Fig. 11. The CH_4 yield on Pt/P25 increases with the increase of the UV irradiation time within

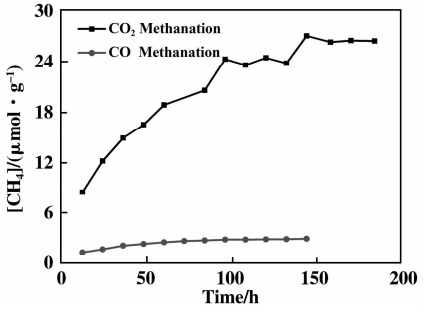

Fig. 11 Variation of CH_4 yield of CO hydrogenation with UV irradiation time over 0.5% Pt/P25 at ambient temperature, $H_2/CO = 3:1$

the first 36 h, subsequently tends to be stable. Compared with CO_2 methanation, the activity of Pt/P25 toward CO methanation is quite lower. According to Katsumi Tanaka[54-55], at room temperature the dissociative adsorption of CO_2 on reduced Pt/TiO_2 can generate CO and chemisorbed oxygen atoms. In our photo experimental results, however, CO is not observed. Considering the fact that Pt/P25 can catalyze CO methanation, thus, it is likely that a small amount of CO is formed and then hydrogenates to produce CH_4 in our experiment. It is generally known that the active sites of reduction reaction over metal supported photocatalyst are metal sites where electrons are trapped. Thus, in

this work, Pt sites are reactive sites providing electrons for activating CO_2 and H_2. Electron excited by the light of UV transmits from the valence band to the conduction band of TiO_2. Owing to the higher work function of Pt-metal than TiO_2, excited electrons transfer from conduction band of TiO_2 to the Pt-metal. H_2 is dissociated to H atoms by Pt. CO_2 is activated by electrons and H atoms on Pt to form formic acid. Because the activity of CO methanation is significantly lower than that of CO_2 methanation. Therefore CO cannot be an important intermediate, only formic acid is important intermediate. It is proposed that photocatalytic CO_2 methanation proceeds *via* formic acid intermediate over Pt/TiO_2. The possible reaction pathway for photocatalytic CO_2 hydrogenation is shown in Fig. 12.

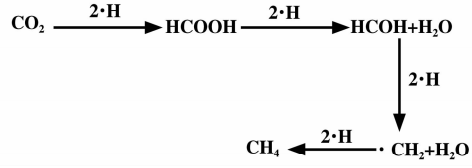

Fig. 12 Reaction pathways of photocatalytic CO_2 hydrogenation

2.3.2 Thermal CO_2 hydrogenation mechanism　Fig. 10 shows at low temperature CO is the main product, at high temperature a large amount of CO transforms into CH_4 and CH_4 becomes the main product. It is supposed that CO is an important intermediate. CO_2-TPD shows that carbonyl Pt appears after Pt loading, which is responsible for the high activity of Pt/P25. This indicates that carbonyl Pt is important intermediate precursor. It is speculated that CO is form carbonyl Pt hydrogenation. Fig. 13 shows the conversion of CO, selectivity and yield of CH_4 and CO_2 over the 0.5% Pt/P25 catalyst at different temperatures. Comparing Fig. 10 with Fig. 13, Pt/P25 catalyst shows a comparable CO_2(CO) conversion, CH_4 selectivity and yield at the same reaction temperature. This means the result of CO_2 hydrogenation is similar to that of CO hydrogenation. It is considered that CH_4 is produced from the hydrogenation of CO, and CO hydrogenation is the rate-determining step.

According to the discussion above, a possible mechanism for CO_2 hydrogenation under the thermal

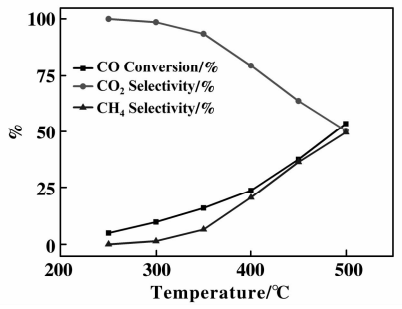

Fig. 13 Conversion of CO, selectivity and yield of CH_4 and CO_2 over the Pt/P25 catalyst at different temperature. $H_2/CO = 3:1$

condition is proposed. Firstly, CO_2 adsorbs on the surface of Pt/P25 catalyst to form carbonyl Pt intermediate precursor, and then transform into CO. Finally, CH_4 is formed *via* CO hydrogenation. The possible reaction pathway for thermal catalytic CO_2 hydrogenation is shown in Fig. 14.

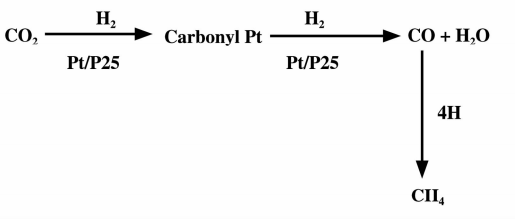

Fig. 14 Reaction pathways of thermal catalytic CO_2 hydrogenation

2.4 Selectivity difference of products of CO_2 hydrogenation under irradiation and thermal condition

In the photocatalytic CO_2 hydrogenation, it shows that loading Pt onto TiO_2 can enhance the production of CH_4. As shown in Fig. 5, the Pt particles on Pt/P25 reduced at 450 ℃ are all in the metallic state. According to our experiment results, P25 is inactive, while Pt/P25 has a higher activity in photocatalytic CO_2 hydrogenation. It is indicated that Pt metal serves as active site. Owing to the higher work function of Pt-metal than TiO_2, excited electrons transmit to the Pt-metal and the recombination between electrons and holes is effectively suppressed. Pt metal highly dispersed on the support shown in Fig. 2 leads to effective active metal surface area, which can promote trapping electrons. For this reason, the electron density on the Pt

particles is increased, which benefits for the formation of CH_4[60]. Pt active sites selectively catalyze CO_2 methanation rather not RWGS. Even though a little CO is produced, it is transformed to CH_4 by enough electrons. As a consequence, photocatalytic CO_2 hydrogenation favors the formation of CH_4 over Pt/TiO_2.

In contrast, in the CO_2 hydrogenation under the thermal condition, at low temperature, CO is the main product, so, the reverse water-gas-shift reaction (RWGS) is the main reaction at low temperature, only a small amount of CO produced can further hydrogenate to CH_4. In our thermal experiment, P25 is inactive in thermal catalytic CO_2 hydrogenation. However, Pt/P25 enhances substantially the reduction of CO_2 with H_2. This suggests that the role of Pt is very important, because Pt activates both CO_2 and H_2. At high temperature, the amount of CH_4 increases, while CO decreases. This indicates CO_2 methanation takes up a large part of the total reaction. The main active sites are Pt sites, and carbonyl Pt is the main intermediate precursor.

Based on the discussion above, it is supposed that different active intermediates work under different reaction conditions. In the photo experiment, excited electrons were trapped by Pt and led to reduction of surface adsorbed carbonyl species to form CH_4 *via* formic acid intermediate. However, under the thermal condition, H_2 was decomposed into H atoms by Pt, adsorbed carbonyl species on Pt surface were reduced by H atoms to form CO, and CO hydrogenated to produce CH_4.

3 Conclusions

The carbon dioxide hydrogenation over these catalysts was investigated under photocatalytic and thermal conditions respectively. Results indicated that hydrogenation of carbon dioxide could be catalyzed by Pt/TiO_2 catalysts, but the reaction occurred in the different ways. Under the thermal condition, CO_2 was converted to CO and CH_4, the main product was CO at low temperature (100% of CO selectivity at 250 ℃ over 0.5% Pt/TiO_2 catalyst). Increase of reaction temperature led to increase of selectivity to CH_4. For example, CH_4 selectivity increased from 0 to 60.94% when reaction temperature was raised from 250 to 450 ℃ over 1.5% Pt/TiO_2 catalyst. The increase of Pt loading resulted in the increase of selectivity of CH_4. On the contrary, methane was the only product under irradiation condition. Reasons resulting in this difference selectivity tendency of products might be as following: It is supposed that different active intermediates work under different reaction conditions. In the photo experiment, excited electrons were trapped by Pt and led to reduction of surface adsorbed carbonyl species to form CH_4 *via* formic acid intermediate. However, under the thermal condition, H_2 was decomposed into H atoms by Pt, adsorbed carbonyl species on Pt surface were reduced by H atoms to form CO, and CO hydrogenated to produce CH_4. It is quite interesting to observe the difference in the selectivity of CO_2 photo and thermal reduction process. In the future, intensive study on this difference will be done to better understand CO_2 hydrogenation.

Acknowledgment

This work is supported by the National Science Foundation of China (21173242), 973 Program and 863 Program of Department of Sciences and Technology of China (Grant Nos. 2012AA051501 and 2013CB632404).

References:

[1] Ghoniem A F. Needs, resources and climate change: Clean and efficient conversion technologies [J]. *Prog Ener Comb Sci*, 2011, **37**: 15-51.

[2] Song C S. Global challenges and strategies for control, conversion and utilization of CO_2 for sustainable development involving energy, catalysis, adsorption and chemical processing [J]. *Catal Today*, 2006, **115**: 2-32.

[3] Olah G A, Surya Prakash G K, Goeppert A. Anthropogenic chemical carbon cycle for a sustainable future [J]. *J Am Chem Soc*, 2011, **133**: 12881-12898.

[4] Zha F, Tian H F, Yan J, *et al*. Multi-walled carbon nanotubes as catalyst promoter for dimethyl ether synthesis from CO_2 hydrogenation [J]. *Appl Surf Sci*, 2013, **285**: 945-951.

[5] Guo J, Ouyang S X, Kako T, *et al*. Mesoporous In(OH)(3) for photoreduction of CO_2 into renewable hydrocarbon fuels [J]. *Appl Surf Sci*, 2013, **280**: 418-423.

[6] Xu X D, Moulijn J A. Mitigation of CO_2 by chemical conversion: plausible chemical reactions and promising products [J]. *Energy Fuels*, 1996, **10**: 305-325.

[7] Wang W, Wang S P, Ma X B. Recent advances in catalytic hydrogenation of carbon dioxide [J]. *Chem Soc Rev*, 2011, **40**: 3703-3727.

[8] Yang H, Xu Z, Fan M, *et al*. Progress in carbon dioxide separation and capture: A review [J]. *J Environ Sci*, 2008, **20**: 14-27.

[9] Mikkelsen M, Jorgensen M, Krebs F C. The teraton challenge. A review of fixation and transformation of carbon dioxide [J]. *Ener Envir Sci*, 2010, **3**: 43-81.

[10] Varghese O K, Paulose M, LaTempa T J. High-rate solar photocatalytic conversion of CO_2 and water vapor to hydrocarbon fuels [J]. *Nano Lett* , 2009, **9**: 731-737.

[11] Inoue T, Fujishima A, Konishi S, *et al*. Photoelectrocatalytic reduction of carbon dioxide in aqueous suspensions of semiconductor powders [J]. *Nature*, 1979, **277**: 637-638.

[12] Thampi K R, Kiwi J, Gratzel M. Methanation ad photomethanation of carbon dioxide at room temperature and atmospheric pressure [J]. *Nature*, 1987, **327**: 506-508.

[13] Kong D. Electrodeposited Ag nanoparticles on TiO_2 nanorods for enhanced UV visible light photoreduction CO_2 to CH_4[J]. *Appl Surf Sci*, 2013, **277**: 105-110.

[14] Feng Yu(封 煜), Liu Xin-yong(刘新勇), Jiang Zhi(江 治), *et al*. Photocatalysis activity of Pt/TiO_2 toward low concentration NO abatement(TiO_2 负载 Pt 对光催化去除低浓度 NO 性能的影响)[J]. *J Mol Catal* (*China*)(分子催化), 2013, **27**: 76-82.

[15] Xie Yan-zhao(谢艳招), Wu Song-hui(吴松辉), Zhao Lin(赵 林), *et al*. Photocatalytic degradation of p-fluorobenzoic acid in sewage over Pt/TiO_2(在 Pt/TiO_2 上光催化降解污水中的对氟苯甲酸)[J]. *J Mol Catal* (*China*)(分子催化), 2012, **26**: 449-455.

[16] Li X K, Zhuang Z J, Li W. Photocatalytic reduction of CO_2 over noble metal-loaded and nitrogen-doped mesoporous TiO_2[J]. *Appl Catal*, *A*: *General*, 2012, **429/430**: 31-38.

[17] Li F F, Wang Z, Yang C, et al. Preparation of Cu/S-TiO_2 photocatalysts and their catalytic activities under visible light [J]. *J Mol Catal* (*China*), 2012, **26**: 174-183.

[18] Cai Li(蔡 莉), Zhang Shu(张 姝). Preparation, characterization and photo-catalytic activities of N-TiO_2 with urea as nitrogen source(尿素为氮源 N-TiO_2 的制备表征及光催化性能)[J]. *J Mol Catal* (*China*)(分子催化), 2012, **26**: 184-191.

[19] Wang C J, Thompson R L, Baltrus J. Visible light photoreduction of CO_2 using CdSe/Pt/TiO_2 heterostructured catalysts [J]. *J Phys Chem Lett*, 2010, **1**: 48-53.

[20] Hu Lei(胡 蕾), Ye Zhi-xiang(叶芝祥), Lu Yuan-gang(卢远刚), *et al*. Preparation of $BiVO_4/TiO_2$ composite photocatalyst and the photocatalytic degradation of sodium humate($BiVO_4/TiO_2$ 复合光催化剂的制备及可见光降解腐殖酸)[J]. *J Mol Catal* (*China*)(分子催化), 2013, **27**: 377-384.

[21] Peng Shao-qin(彭绍琴), Liu Xiao-yan(刘晓燕), Ding Min(丁 敏), *et al*. Preparation of CdS-Pt/TiO_2 composite and the properties for splitting sea water into hydrogen under visible light irradiation(复合光催化剂 CdS-Pt/TiO_2 制备及可见光光解海水制氢性能)[J]. *J Mol Catal* (*China*)(分子催化), 2013, **27**: 459-466.

[22] Li Jin-li(李锦丽), Fu Ning(付 宁), Lu Gong-xuan(吕功煊). Photocatalytic methanation of CO_2 over TiO_2 nanoribbons(TiO_2 纳米带光催化二氧化碳甲烷化)[J]. *Chin J Inorg Chem*(无机化学学报), 2010, **26**: 2175-2181.

[23] Tsai C C, Nian J N, Teng H. Mesoporous nanotube aggregates obtained from hydrothermally treating TiO_2 with NaOH [J]. *Appl Surf Sci*, 2006, **253**: 1898-1902.

[24] Rani S, Bao N, Roy S C. Solar spectrum photocatalytic conversion of CO_2 and water vapor into hydrocarbons using TiO_2 nanoparticle membranes [J]. *Appl Surf Sci*, 2014, **289**: 203-208.

[25] He Xue-zhi(贺学智), Li Bing-jie(李炳杰), Wu Zhi-jian(吴志坚), *et al*. The preparation of layered double metals hydroxides Zn (Cu)/Al-LDHS and the photocatalytic reduction of CO_2(层状双金属氢氧化物 Zn (Cu)/Al-LDHS 的制备及其光催化还原二氧化碳的研究)[J]. *J Mol Catal* (*China*)(分子催化), 2013, **27**: 70-75.

[26] Zhu Li-xiao(朱力校), Zhao Zhi-huan(赵志换), Yue Xue-yong(岳学勇), *et al*. One-pot hydrothermal synthesis of Ag@ Ag_2S modified porous TiO_2 and its photocatalytic and antimicrobial properties(一步法制备银-硫化银负载多孔 TiO_2 及其光催化和抗菌性能)[J]. *J Mol Catal* (*China*)(分子催化), 2013, **27**: 465-473.

[27] Xie S J, Wang Y, Zhang Q H, *et al*. Photocatalytic reduction of CO_2 with H_2O: significant enhancement of the activity of Pt-TiO_2 in CH_4 formation by addition of MgO [J]. *Chem Commun*, 2013, **49**: 2451-2453.

[28] Lo C C, Hung C H, Yuan C S. Photoreduction of carbon

dioxide with H_2 and H_2O over TiO_2 and ZrO_2 in a circulated photocatalytic reactor [J]. *Sol Ener Mater Sol Cells*, 2007, **91**: 1765-1774.

[29] Zhang Q H, Han W D, Hong Y J. Photocatalytic reduction of CO_2 with H_2O on Pt-loaded TiO_2 catalyst [J]. *Catal Today*, 2009, **148**: 335-340.

[30] Yu K P, Yu W Y, Kuo M C, *et al*. Pt/titania-nanotube: a potential catalyst for CO_2 adsorption and hydrogenation [J]. *Appl Catal B: Environm*, 2008, **84**: 112-118.

[31] Kim S S, Park K H, Hong S C. A study of the selectivity of the reverse water-gas-shift reaction over Pt/TiO_2 catalysts [J]. *Fuel Proc Tech*, 2013, **108**: 47-54.

[32] Karelovic A, Ruiz P. Mechanistic study of low temperature CO_2 methanation over Rh/TiO_2 catalysts [J]. *J Catal*, 2013, **301**: 141-153.

[33] Yamasaki M, Habazaki H, Asami K. Effect of tetragonal ZrO_2 on the catalytic activity of Ni/ZrO_2 catalyst prepared from amorphous Ni-Zr alloys [J]. *Catal Comm*, 2006, **7**: 24-28.

[34] Tang L P, Zhang H T, Li M L, *et al*. Combination-type MgO/CNTs composites as effective supports for CO hydrogenation to light olifin [J]. *J Mol Catal (China)* (分子催化), 2012, **26**: 391-398.

[35] Zhang Yan-xin (张颜鑫), Zhang Yin (张 因), Zhao Yong-xiang (赵永祥). Effect of ZrO_2 polymorphs on catalytic performance of Ni/ZrO_2 catalysts for CO methanation (ZrO_2 晶型对 Ni/ZrO_2 催化剂 CO 甲烷化性能的影响) [J]. *J Mol Catal (China)* (分子催化), 2013, **27**: 349-355.

[36] Abe T, Tanizawa M, Watanabe K, *et al*. CO_2 methanation property of Ru nanoparticle-loaded TiO_2 prepared by a polygonal barrel-sputtering method [J]. *Ener Envir Sci*, 2009, **2**: 315-321.

[37] Zhang Ya-jing (张雅静), Deng Ju-lei (邓据磊), Zhang Su-juan (张素娟), *et al*. Investigation on CuO-ZnO-Al_2O_3/HZSM-5 catalysts for synthesis of dimethyl ether from CO_2 hydrogenation (CO_2 加氢制备二甲醚 CuO-ZnO-Al_2O_3/HZSM-5 催化剂的研究) [J]. *J Mol Catal (China)* (分子催化), 2013, **27**: 235-241.

[38] Park J N, McFarland E W. A highly dispersed Pd-Mg/SiO_2 catalyst active for methanation of CO_2 [J]. *J Catal*, 2009, **266**: 92-97.

[39] Jacquemin M, Beuls A, Ruiz P. Catalytic production of methane from CO_2 and H_2 at low temperature: Insight on the reaction mechanism [J]. *Catal Today*, 2010, **157**: 462-466.

[40] Marwood M, Doepper R, Renken A. In-situ surface and gas phase analysis for kinetic studies under transient conditions, The catalytic hydrogenation of CO_2 [J]. *Appl Catal A: Gener*, 1997, **151**: 223-246.

[41] Schild C, Wokaun A, Baiker A. On the mechanism of CO and CO_2 hydrogenation reactions on zirconia-supported catalysts: a diffuse reflectance FTIR study Part II. Surface species on copper/zirconia catalysts: implications for methanol synthesis selectivity [J]. *J Mol Catal*, 1990, **63**: 243-254.

[42] Wu Yu-qi (吴玉琪), Lu Gong-xuan (吕功煊), Li Shuben (李树本). Hydrogen production by Pt/TiO_2 anaerobic photocatalytic reforming degradation of aqueous monoethanolamine (无氧条件下 Pt/TiO_2 光催化重整降解一乙醇胺水溶液制氢) [J]. *Acta Phys-Chim Sin* (物理化学学报), 2004, **20**: 755-758.

[43] Li Bo (李 波), Lu Gong-xuan (吕功煊). Cosensitized TiO_2 with different dyes for water splitting to hydrogen under visible light-structural similarity of dyes and their dual promoting effect (不同染料共敏化 TiO_2 可见光分解水产氢性能研究-染料结构相似性与双重促进效应) [J]. *J Mol Catal (China)* (分子催化), 2013, **27**: 181-191.

[44] Wu Xiao-man (武小满), Jin Xiao-jing (靳小静), Guo Li-li (郭丽丽). Preparation and photocatalytic properties of nano-TiO_2 by hydrothermal method with template (模板水热法纳米 TiO_2 制备及光催化性能研究) [J]. *Chem Res and Appl* (化学研究与应用), 2012, **24**: 901-905.

[45] Keller V, Bernhardt P, Garin F. Photocatalytic oxidation of butyl acetate in vapor phase on TiO_2, Pt/TiO_2 and WO_3/TiO_2 catalysts [J]. *J Catal*, 2013, **215**: 129-138.

[46] Fu N, Lu G X. Photo-catalytic H_2 evolution over a series of Keggin-structure heteropoly blue sensitized Pt/TiO_2 under visible light irradiation [J]. *Appl Surf Sci*, 2009, **255**: 4378-4383.

[47] Zhang X J, Li J L, Lu G X. Visible light induced CO_2 reduction and Rh B decolorization over electrostatic-assembled AgBr/palygorskite [J]. *J Colloid Interface Sci*, 2012, **377**: 277-283.

[48] Rajalakshmi K. Photocatalytic reduction of carbon dioxide in conjunction with decomposition of water on oxide semiconductor surfaces [D]. Department of Chemical Engineer Indian Institute of Technology, Madras, May, 2011.

[49] Yu J G, Yu H G, Cheng B. Enhanced photocatalytic activity of TiO_2 powder (P25) by hydrothermal treatment [J]. *J Mol Catal A: Chemical*, 2006, **253**: 112-118.

[50] Spurr R A, Myers H. Quantitative analysis of anatase-rutile mixtures with an X-Ray diffractometer [J]. *Anal Chem*, 1957, **29**: 760.

[51] Wagner C D, Riggs W M, Moulder J F. *Handbook of X-ray Photo-electron Spectroscopy* [S], Perkin Elmer Corporation, USA, 1992.

[52] Baumgarten E, Fiebes A, Stumpe A. Synthesis and characterization of a new platinum supported catalyst based on poly-(acrylamide-co-[3-(acryloylamino) propyltrimethylammoniumchloride]) as carrier [J]. *J Mol Catal A-Chem*, 1996, **113**: 469-477.

[53] Kim S S, Lee H H. A study on the effect of support's reducibility on the reverse water-gas shift reaction over Pt catalysts [J]. *Appl Catal A: General*, 2012, **423/424**: 100-107.

[54] Tanaka K, Miyahara K, Toyoshima I. Adsorption of CO_2 on TiO_2 and Pt/TiO_2 studied by X-ray photoelectron spectroscopy and auger electron spectroscopy [J]. *J Phys Chem*, 1984, **88**: 3504-3508.

[55] Tanaka K, White J M. Dissociative adsorption of CO_2 on oxidized and reduced Pt/TiO_2[J]. *J Phys Chem*, 1982, **86**: 3977-3980.

[56] Amy L L, Lu G G, John T. Photocatalysis on TiO_2 surfaces: principles, mechanisms, and selected results [J]. *Chem Rev* 1995, **95**: 735-758.

[57] Goguet A, Meunier F C, Tibiletti D. Spectrokinetic investigation of reverse water-gas-shift reaction intermediates over a Pt/CeO_2 catalyst [J]. *J Phys Chem B*, 2004, **108**: 20240-20246.

[58] Panagiotopoulou P, Kondarides D I. A comparative study of the water-gas shift activity of Pt catalysts supported on single (MO_x) and composite (MO_x/Al_2O_3, MOx/TiO_2) metal oxide carriers [J]. *Catal Today*, 2007, **127**: 319-329.

[59] Panagiotopoulou P, Christodoulakis A, Kondarides D I, *et al.* Particle size effects on the reducibility of titanium dioxide and its relation to the water-gas shift activity of Pt/TiO_2 catalysts [J]. *J Catal*, 2006, **240**: 114-125.

[60] Zhai Q G, Xie S J, Fan W Q. Photocatalytic conversion of carbon dioxide with water into methane: platinum and copper(I) oxide co-catalysts with a core-shell structure [J]. *Angew Chem Int Ed*, 2013, **52**: 5776-5779.

光照和加热条件下 Pt/TiO_2 催化二氧化碳加氢

陈术清[1,2]，吕功煊[1*]

（1. 中科院兰州化学物理研究所 羰基合成与选择氧化国家重点实验室，甘肃 兰州 730000；2. 中国科学院大学，北京 100080）

摘要： 浸渍法制备了 Pt 负载量为 0.5 to 2% 的 Pt/TiO_2 催化剂，考察它们在光照和加热条件下二氧化碳催化加氢性能. 结果表明，二氧化碳加氢反应均可在 Pt/TiO_2 的催化下进行，但在不同反应条件下加氢反应通过不同方式进行. 在加热条件下，二氧化碳可转化为一氧化碳和甲烷，且在低温加热条件下一氧化碳是主产物（CO 选择性为 100%，250 ℃，0.5% Pt/TiO_2）. 在 1.5% Pt/TiO_2 催化剂上，当反应温度从 250 ℃升高到 450 ℃时，CH_4 的选择性由 0 增加到 60.94%. 同时，增加 Pt 的负载量也会导致 CH_4 的选择性的增加. 然而，在光照条件下，产物只有甲烷. CO_2-TPD 结果表明，二氧化碳通过羰基基团与作为吸附中心的 Pt 相连接. 结合催化活性与表征结果，提出在光照条件下，反应可能以二氧化碳和氢气分别被光生电子活化反应生成甲酸中间体，随后经由甲酸加氢和脱水生成甲烷的机理进行. 而在加热条件下，反应可能以二氧化碳首先吸附在催化剂表面形成羰基 Pt 物种，随后加氢生成一氧化碳，一氧化碳继续加氢生成甲烷的机理进行.

关键词： 光催化；热催化；CO_2 加氢